Atmospheric Environment 218 (2019) 116998

Contents lists available at ScienceDirect

Atmospheric Environment

journal homepage: http://www.elsevier.com/locate/atmosenv

Quantifying depression trapping effect on rainwater chemical composition during the rainy season in karst agricultural area, southwestern China

Jie Zeng [a], Fu-Jun Yue [b,c,d,e,*], Zhong-Jun Wang [e,f], Qixin Wu [g], Cai-Qing Qin [b], Si-Liang Li [b,d,e]

[a] Institute of Earth Sciences, China University of Geosciences (Beijing), Beijing, 100083, China
[b] Institute of Surface-Earth System Science, Tianjin University, Tianjin, 300072, China
[c] School of Geographical and Earth Sciences, University of Glasgow, Glasgow, G12 8QQ, United Kingdom
[d] Tianjin Key Laboratory of Earth Critical Zone Science and Sustainable Development in Bohai Rim, Tianjin University, Tianjin, 300072, China
[e] Puding Karst Ecosystem Research Station, Institute of Geochemistry, Chinese Academy of Sciences, Anshun, 562100, China
[f] State Key Laboratory of Environmental Geochemistry, Institute of Geochemistry, Chinese Academy of Sciences, Guiyang, 550081, China
[g] Key Laboratory of Karst Environment and Geohazard, Ministry of Land and Resources, Guizhou University, Guiyang, 550025, China

HIGHLIGHTS

- The vertical variation of rainwater chemistry in karst valley area was evaluated.
- The ions sources and controlling factors were explored at two altitude sites.
- $\delta^{15}N–NO_3$ shown relatively high soil NO_X contribution at depression site.
- The depression trapping effect was highly impacted on Ca^{2+} and NH_4^+.

ARTICLE INFO

Keywords:
Major ions
Rainwater
Wet deposition rate
Nitrate isotopes
Karst
Depression trapping effect

ABSTRACT

Atmospheric wet deposition is a vital part of biogeochemical cycles in earth surface environment systems, which is not only controlled by local sources and long-range transported continental substances from natural and anthropogenic sources, but also potentially influenced by the topographical features (e.g. peak clusters and depressions in karst areas). To investigate the depression trapping effect of vertical distribution of rainwater chemical composition and evaluate the effect of trapping by depression on wet deposition flux, rainwater samples from two sites (HR, a hilltop shrubbery area, and LR, inside a depression paddy field area) of a karst agricultural depression in Southwest China, were collected during the rainy season. From these, the major ionic concentrations were measured. The results indicated a variance in pH from 4.8 to 6.4 with a volume-weighted mean (VWM) value of 5.7 at the HR, and, a range of 5.4–6.9 with a VWM of 6.0 at the LR. The VWM concentrations of ions were decreased in the order of $SO_4^{2-} > NH_4^+ > Ca^{2+} > NO_3^- > Mg^{2+} > K^+ > Na^+ > Cl^- > F^-$ at both sites, and were dominated by SO_4^{2-}, NH_4^+, Ca^{2+}, and NO_3^-, accounting for >87% of the total ions at the two sites. The result of fractional acidity (FA) and neutralization factors (NF) revealed that the relatively high pH values were the result of neutralization of the alkaline substances (NH_4^+ and Ca^{2+}) rather than the scarcity of acidic materials. Source analysis of major ions showed that anions were predominantly controlled by anthropogenic emission, while cations originated from both terrestrial sources and anthropogenic activity. The vertical distribution of dominant ions (NH_4^+, NO_3^-, Ca^{2+}, Mg^{2+}, and SO_4^{2-}) were ascribed to the relatively weak air convection movement within the depression area (specific atmospheric circulations) and the differences in human interference at two sites (LR, cultivated land; HR, luxuriant vegetation). This is further supported by the more negative rainwater $\delta^{15}N–NO_3^-$ values (−8.5 to −6.0‰), in LR than that in HR (−6.2 to −3.4‰). The depression trapping effect could significantly affect the estimation of wet deposition fluxes (up to 80.6% for Ca^{2+} and 68.7% for NH_4^+), which requires consideration in future studies, e.g. N wet deposition.

* Corresponding author. Institute of Surface-Earth System Science, Tianjin University, Tianjin, 300072, China.
E-mail address: fujun_yue@tju.edu.cn (F.-J. Yue).

https://doi.org/10.1016/j.atmosenv.2019.116998
Received 15 July 2019; Received in revised form 18 September 2019; Accepted 19 September 2019
Available online 20 September 2019
1352-2310/© 2019 Elsevier Ltd. All rights reserved.

1. Introduction

In recent decades, atmospheric pollution has increased dramatically with rapid economic and social development. This is particularly significant in China as the biggest developing country (Hao et al., 2001; Larssen et al., 2006; Wu and Han, 2015). The high atmospheric concentrations of anthropogenic and natural materials, such as SO_x, NO_x, and fine particulate matter, have significantly impacted the global ecosystem material cycle and seriously threaten human life and health (Larssen et al., 2006; Galloway et al., 2008; Tao et al., 2014; Rao et al., 2017; Wei et al., 2019). Therefore, air pollution (e.g., windblown dust, acid rain, haze, and smog) has increasingly become a significant scientific issue in China (Wu et al., 2012; Rao et al., 2017).

The water chemistry of rainwater is an effective indicator for the evaluation of atmospheric environment quality. Generally, SO_4^{2-} and NO_3^- in rainwater are considered to be of primarily anthropogenic origin (the dissolution of precursor gases such as SO_x and NO_x from fossil fuel combustion), while the cations, including Ca^{2+}, Mg^{2+}, and K^+, are assumed to be mainly from terrestrial sources. Na^+ and Cl^- are sea-salt ions. NH_4^+ is the product of the NH_3, captured by rainwater from agricultural activity (Han et al., 2010; Xiao et al., 2013; Xu et al., 2015; Lü et al., 2017).

The chemical characteristics of rainwater, including pH distribution, sulfur deposition and nitrogen deposition in urban areas of China, has been widely studied (Xiao and Liu, 2002; Han and Liu, 2006; Zhang et al., 2012; Xiao et al., 2013; Yu et al., 2015; Rao et al., 2017; Zhou et al., 2019), but has rarely been reported in rural areas (Zhao et al., 2008; Wu et al., 2012; Lü et al., 2017). Additionally, several studies have compared the spatial distribution of rainwater chemical composition and ionic deposition fluxes on a large scale (Xiao et al., 2014; Xu et al., 2015; Rao et al., 2017), while there are few studies from a small scale perspective. Previous studies have shown that the variations of rainwater chemistry are influenced by many factors, including meteorological factors, orographic barriers, anthropogenic factors that influence the precipitation chemistry (Szép et al., 2018; Han et al., 2019). Among these factors, the orographic barriers factor is rare studied. Szép et al. (2019) concluded that the rainwater chemistry was significantly influenced in intra-mountain basins with specific atmospheric circulations.

The typical karst geomorphology in Southwest (SW) China is depression, cone, and cockpit with thin and barren soil, where the underlying surface changes diversely. In such orographic conditions (e.g. karst peak clusters with many depressions), the local atmospheric circulations can also cause the variations of rainwater chemistry. Moreover, due to the special geological background and intense karstification, the subterranean and surface streams are connected through karst sinkholes in this area, and the rainfall could accelerates the transportation of substances between the underground and surface via runoff and caused the extremely severe soil erosion (Zeng et al., 2019). This is problematic as the karstic ecosystem is extremely sensitive. Comparing to the solutes flux origin from soil erosion, rainfall give a small contribution to solutes flux in aquatic environment (Xiao et al., 2015; Gao et al., 2017). However, rainfall can accelerate the transport of element migration on the surface of karst areas and contribute solute to the surficial ecosystem in the form of wet deposition (Hao et al., 2017; Dai et al., 2018; Yan et al., 2018). Thus, wet deposition (rainwater) is important to the development of an ecosystem and is an important participant in rock weathering, which directly affects the structure and function of the ecosystem and hydrochemical compositions in karst areas (Lee et al., 2012; Yue et al., 2015).

Additionally, the climate in southwest of China was controlled by a subtropical monsoon climate with concentrated rainstorm events occurring in the wet season (Yue et al., 2018), concentrated rainfall events result in rapid leaching of nutrients in the epikarst system due to weak water holding capacity (Song et al., 2017; Ma et al., 2018). Consequently, the karstic ecosystem is vulnerable and it is necessary to enhance our knowledge of rainwater chemical composition in the wet season for better water quality management and better understand the geochemical cycle in karstic agricultural areas. This study presents the rainy season data from an initial collection of chemical characteristics from rainwater collected at two different altitude sites (located on a hilltop and in a depression) in a karst agricultural depression (SW China). The objectives of this study are to: 1) explore the cause of acid neutralization in rainwater; 2) identify the possible sources of major ions in rainwater; 3) analyse the controlling factor(s) of ionic vertical distribution and, 4) quantify the depression trapping effect on wet deposition fluxes in the karst peak clusters and depressions geomorphology.

2. Materials and methods

2.1. Site description

The study area is located in the Puding Karst Critical Zone Observatory, in the upper reaches of the Dengzhan River, which is one of the seasonal streams in the Houzhai Catchment (Guizhou province, Southwest China) (Fig. 1).

This area is characterized by a subtropical, monsoonal climate, with an average annual temperature 15.1 °C. Annual precipitation generally ranges from 1200 to 1400 mm, where a majority of annual rainfall (~80%) occurs between May and October (Wu et al., 2012; Yue et al., 2018). The lithology in the study area is composed of limestone and dolomite of the Permian and Triassic ages (Chen et al., 2008; Zhang et al., 2017; Zhao et al., 2018). The depression is surrounded by mountains on three sides with the highest mountain in the whole basin (Tianlong mountain) located in the east of the depression (Fig. 1). The total area of the depression is about 1.5 km^2 with three kinds of land cover/use (paddy fields, drylands, and shrubbery, Fig. 1) (Zhao et al., 2018). Two sites were selected to collect rainwater samples: high altitude rainfall site (HR, 105°45′49″ E, 26°14′45″ N, 1550 m asl.) located at the highest altitude of the studied catchment, on the top of Tianlong hill surround by shrubbery, and the low altitude depression site (LR, 105°45′29″ E, 26°15′06″ N, 1290 m asl.) located in the farmland area (Fig. 1). The main crops of the studied area are rice and corn in the summer season (May to August), while rapeseed is the major crop in the winter season. Most fertilizers, including urea, di-ammonium phosphate and organic fertilizers, are applied during the summer season, while only a fraction of fertilizer is used during the winter season.

2.2. Sample collection

A polyethylene sampler (65 cm diameter), placed approximately

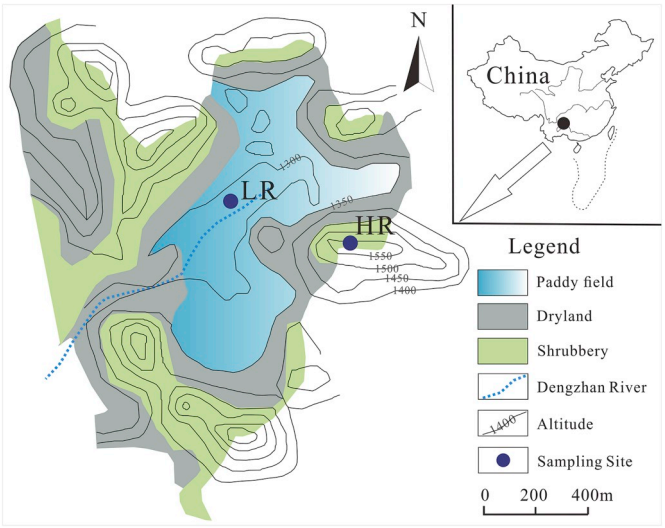

Fig. 1. The land use of the area studied. Map modified from Zhao et al. (2018).

100 cm above the ground, was used to collect rainwater samples. In order to avoid the effects of atmospheric fine particle deposition in the absence of rainfall, a polyethylene cap was applied to cover the sampler, and the cap was removed as quickly as possible when it began to rain. The rainwater samples were collected daily (one sample was collected every 24 h if the rainfall event lasts longer than one day) at two sites. A total of 38 (19 samples form HR and 19 samples form LR) rainwater samples were collected during the rainy season (May to August 2015).

2.3. Analysis and calculation

Electrical conductivity (EC) and pH were immediately measured by a portable multiple parameter (WTW, Multi Line 3320) after sampling. The rainwater samples were then filtered through 0.45 μm acetate membrane filters, and the filtrate was stored directly in a pre-cleaned polyethylene bottle for measurement of ion concentration and nitrate isotopes. All the rainwater samples were kept refrigerated at 4 °C until analysis. The NH_4^+ and NO_3^- concentration in rainwater samples were analyzed by using a continuous-flow analyzer (Skalar, SAN^{++}), and the remaining ions (K^+, Na^+, Ca^{2+}, Mg^{2+}, F^-, Cl^-, and SO_4^{2-}) concentration were measured by ionic chromatography (Thermo Fisher, ICS-Aquion 1100) in the Institute of Geochemistry, Chinese Academy of Sciences. Reagent and procedural blanks with the identical treatments to the sample were also analyzed to perform the method validation and quality control. The analytical precision for ionic concentration is ~ ± 5%. Nitrate isotopes (expressed in delta notation, $\delta^{15}N_{nitrate}$) were measured through the denitrifier method (McIlvin and Casciotti, 2011) using an isotope ratio mass spectrometer (IsoPrime, GV, UK). The international reference materials were used for calibration of $\delta^{15}N_{nitrate}$. The analytical precision of $\delta^{15}N$ for nitrate was better than ±0.3‰.

The volume-weighted mean (VWM) values of the parameters (pH, EC, and ion concentration) are calculated with the equation (1):

$$C = \frac{\sum C_i P_i}{\sum P_i} \quad (1)$$

where C is the VWM values of the parameters, C_i is the concentration (pH or EC value) of the samples, i is the number of samples, P_i is the daily rainfall amount corresponding to the sample. The data of daily rainfall amount during the sampling period are from the China Weather Net (http://www.weather.com.cn/).

To identify the extent to which rainwater acidity is neutralized by the cations, the fractional acidity (FA) of the two main acidic components in rainwater (SO_4^{2-} and NO_3^-) is calculated as equation (2) (Balasubramanian et al., 2001):

$$FA = \frac{[H^+]}{[SO_4^{2-}] + [NO_3^-]} \quad (2)$$

where H^+, SO_4^{2-}, and NO_3^- are the corresponding ion concentrations expressed in μeq/L. If FA = 1, the neutralization of the rainwater acidity will not be completed at all (Wu et al., 2012).

To assess the neutralization of rainwater by each cation, the neutralization factors (NF) are also applied and calculated in equation (3) (Possanzini et al., 1988):

$$NF_{Xi} = \frac{[X_i]}{[SO_4^{2-}] + [NO_3^-]} \quad (3)$$

where X_i is the concentrations of cations (expressed in μeq/L).

3. Results and discussion

3.1. Ionic composition and acid neutralization of rainwater

The detailed data for each sample is shown in Table S1. The ionic concentration, EC and pH values of the rainwater samples, along with the rainfall amounts, are statistically listed in Table 1 and are plotted in Fig. 2. The concentrations of each ion show high dispersions around their mean values with large standard deviations (Table 1) indicating a large variation of the ion concentrations over the rainfall event. The VWM concentrations of ions are decreased in the following order: $SO_4^{2-} > NH_4^+ > Ca^{2+} > NO_3^- > Mg^{2+} > K^+ > Na^+ > Cl^- > F^-$ at both sites (Table 1). SO_4^{2-}, NH_4^+, Ca^{2+}, and NO_3^- in rainwater are the dominant, accounting for >87% (average) of the total ions at the two sites. Compared with other areas (Table 2), most of ion concentrations of HR and LR are neither higher than those studies conducted in city areas such as Guiyang, Beijing, Xi'an, Dalian, and Chengdu (Han and Liu, 2006; Lu et al., 2011; Wang and Han, 2011; Zhang et al., 2012; Xu et al., 2015) nor higher than those observed in desert regions, rural areas, remote areas, mountain areas, oceanic islands and the Bohemian karst area (Li et al., 2007; Špičková et al., 2008; Zhao et al., 2008; Wu et al., 2012; Xiao et al., 2016; Rao et al., 2017).It is note to worth that the SO_4^{2-}, NO_3^-, and NH_4^+ concentrations of HR and LR are higher than those observed in East Tianshan (mountain area), Tibet (remote area), and Yongxing island (oceanic island) (Li et al., 2007; Zhao et al., 2008; Xiao et al., 2016). This indicates that the rainwater in the study area is more affected by human activity (e.g., anthropogenic SO_x, NO_x, and NH_3), compared to remote mountain areas and on oceanic islands.

The VWM EC values of HR and LR are 10.6 and 16.0 μS/cm (Table 1), respectively. The total cation concentrations ($TZ^+ = K^+ + Na^+ + Ca^{2+} + Mg^{2+} + NH_4^+$) range greatly from 13.9 to 124.8 μeq/L at the HR and from 31.4 to 333.9 μeq/L at the LR (Table S1), while the total anion concentrations ($TZ^- = F^- + Cl^- + SO_4^{2-} + NO_3^-$) varies from 8.7 to 106.8 μeq/L at the HR and from 27.0 to 218.1 μeq/L at the LR (Table S1). Most of the rainwater samples have TZ^+ higher than TZ^- at the two sites (Fig. S1).

The observed imbalance between cations and anions indicates that there are some unmeasured inorganic or organic anionic species such as HCO_3^- (dissolved the atmospheric CO_2), and oxalate (e.g., released from the vegetation leaves or soil) (Mouli et al., 2005; Han et al., 2010; Rao

Table 1
Statistical results of rainfall amounts (mm/d), pH, EC (μS/cm) and ion concentrations (μeq/L) in rainwater samples of karst depression in the rainy season.

Site	Item	RA	pH	EC	K^+	Na^+	Ca^{2+}	Mg^{2+}	NH_4^+	F^-	Cl^-	SO_4^{2-}	NO_3^-
HR	Mean	28.8	5.8	11.0	3.4	2.9	28.7	6.4	32.1	1.2	2.2	40.2	15.7
n = 19	Median	23.1	6.0	10.9	3.8	2.6	21.9	6.2	28.5	1.2	2.4	50.4	12.5
	SD	26.5	0.5	4.8	1.6	2.6	19.6	4.0	19.1	0.7	1.0	23.3	11.1
	Min	0.9	4.8	3.4	0.5	0.0	3.9	0.1	5.7	0.3	0.4	7.2	1.1
	Max	99.0	6.4	18.7	6.3	10.9	63.8	11.6	63.9	2.4	3.6	81.6	36.8
	VWM	–	5.7	10.6	3.4	3.1	27.0	5.6	30.9	1.1	2.4	36.8	17.7
LR	Mean	28.8	6.0	19.3	5.6	3.3	60.9	7.9	56.2	1.6	2.9	65.3	23.0
n = 19	Median	23.1	6.0	18.4	4.7	2.4	42.2	8.2	52.6	1.4	2.3	64.2	14.5
	SD	26.5	0.4	7.9	4.2	2.5	46.5	5.3	27.6	0.9	2.6	37.6	18.5
	Min	0.9	5.4	8.2	1.0	0.7	8.0	1.2	18.7	0.5	0.9	19.3	5.6
	Max	99.0	6.9	39.0	18.6	10.2	190.1	19.5	115.0	3.3	11.7	160.0	59.3
	VWM	–	6.0	16.0	4.3	2.6	48.7	6.3	52.1	1.6	2.0	54.7	17.0

Note: RA, SD and VWM refer to rainfall amount, standard deviation and volume-weighted mean, respectively.

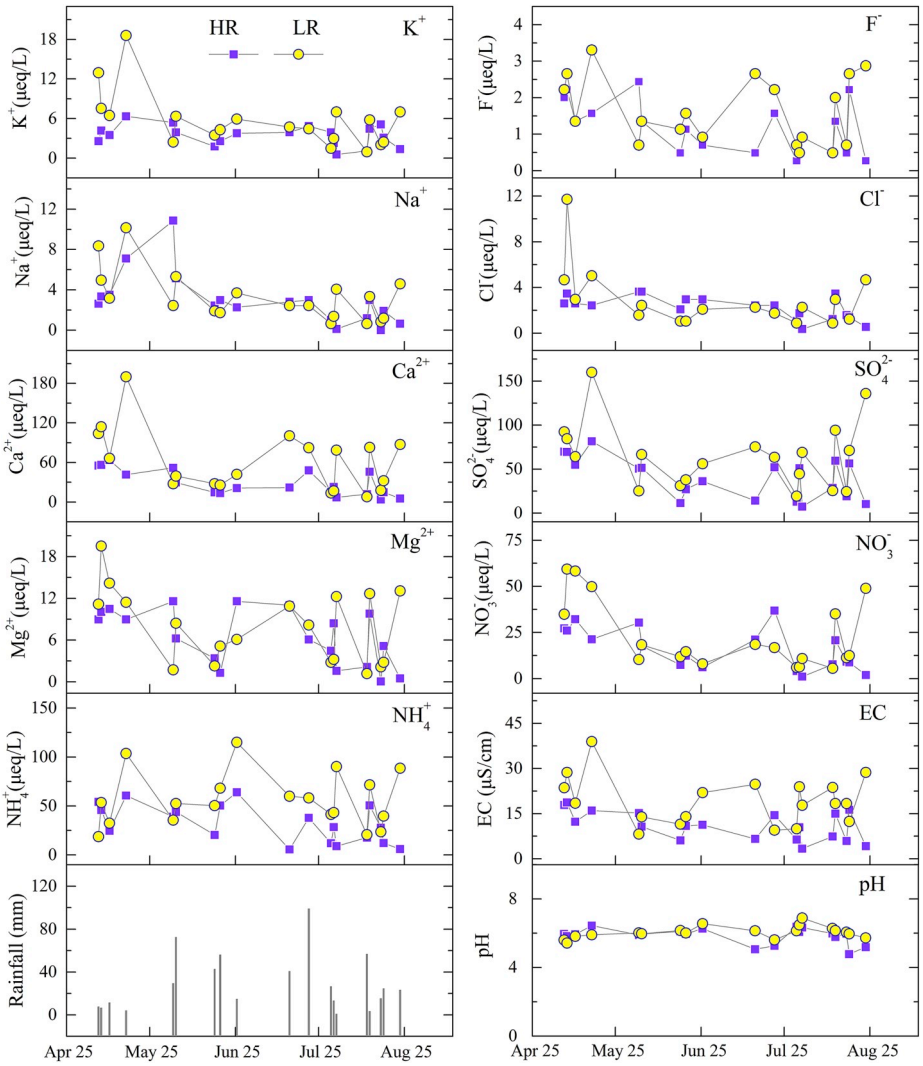

Fig. 2. The pH, EC, ionic concentrations and amount of rainfall in the karst depression in the rainy season.

Table 2
The VWM values (μeq/l) of major ions in rainwater at the karst depression and other places.

Site	pH	K^+	Na^+	Ca^{2+}	Mg^{2+}	NH_4^+	F^-	Cl^-	SO_4^{2-}	NO_3^-	Rainwater type	Reference
HR	5.7	3.4	3.1	27.0	5.6	30.9	1.1	2.4	36.8	17.7	Karst depression	This study
LR	6.0	4.3	2.6	48.7	6.3	52.1	1.6	2.0	54.7	17.0	Karst depression	This study
Guiyang*	4.5	11.0	4.0	113.2	25.5	–	–	21.2	188.0	48.2	Karst city	Han and Liu (2006)
Maolan	5.4	3.5	2.4	20.8	3.0	30.2	0.9	5.1	40.4	3.0	Karst forest	Han et al. (2010)
Beijing	4.9	9.2	21.5	273.0	53.3	346.0	12.0	50.9	357.0	42.6	Megacity	Xu et al. (2015)
Xi'an	6.6	13.8	31.1	425.6	36.6	229.8	28.7	38.7	489.7	128.8	City	Lu et al. (2011)
Dalian	4.8	6.9	36.2	78.9	25.3	107.8	11.3	59.8	168.0	51.4	City	Zhang et al. (2012)
Chengdu	5.1	6.6	1.4	393.2	32.4	150.5	6.2	8.9	425.6	156.2	City	Wang and Han (2011)
Alxa desert	7.6	34.1	232.5	663.0	72.1	167.2	–	202.8	471.4	69.7	Desert	Rao et al. (2017)
Puding	5.7	9.1	10.8	155.8	3.9	33.1	–	13.9	152.4	17.0	Rural	Wu et al. (2012)
Eastern Tien Shan	7.0	4.0	19.0	174.2	18.1	25.2	–	16.5	53.0	9.6	Mountain area	Zhao et al. (2008)
Tibet*	6.6	14.5	15.4	65.6	7.4	18.1	–	19.2	15.5	10.4	Remote	Li et al. (2007)
Yongxing island	–	5.8	209.7	128.8	45.6	8.7	–	214.4	38	8.9	Oceanic island	Xiao et al. (2016)
Prague	6.0	23.4	8	319.9	10.3	–	2.7	18.3	129	72.9	Bohemian karst	Špičková et al. (2008)

Note: * means the data are mean values — means no data.

et al., 2015). However, the pH values of rainwater are less than 6.6 (median value 6.0, Table 1), and the HCO_3^- will be neutralized. Thus, the ion imbalance could be supported by the high contribution rate (12.6%) of organic acid to the rainwater anions (Zhang et al., 2011). Moreover, the sampling period of this study was the rainy season, and the crops (e.g., paddy) and natural plants (e.g., shrubs) thrive with the benefit of intense photosynthesis (Liu et al., 2016), benefiting the release of organic acid into the atmosphere.

The VWM pH value of rainwater is 5.7 at the HR, which is slightly lower than that of LR (6.0) (Table 1 and Fig. 2). As the result of atmospheric CO_2, NO_x, and SO_2 in clouds and raindrops, the pH values of rainwater in the clean atmosphere should be between 5.0 and 5.6

(Galloway et al., 1993; Wu et al., 2012).

Although the study site was defined as an acid rain control zone (central part of Chongqing–Guiyang–Liuzhou zone) in the early 20th century (Hao et al., 2001), the acid deposition (e.g., SO_4^{2-}) in this karst areas of Southwest China has shown a decreasing trend due to the implementation of environmental protection policies, such as in sulfur dioxide reduction (Wu et al., 2012; Lü et al., 2017). Approximately 79% of the rainwater samples had pH values higher than 5.6 in the study area (Table S1), which indicates inputs of alkaline substances into the rainwater. The relatively high pH of rainwater samples observed here is probably caused by the dissolution of NH_3 (g) and windblown dust, originating from agricultural soil emission and dry deposition with a high $CaCO_3$ and $MgCO_3$ content in the karst area (Tang and Han, 2019). Therefore, the pH value reported here is higher than that observed at other karst city or forest sites (Table 2), in Southwest China (Han and Liu, 2006; Han et al., 2010). Nevertheless, the pH in this study is far lower than that observed in desert areas extremely affected by dust (Table 2), as in northwest China (Rao et al., 2017).

The relatively high-pH values and dominant SO_4^{2-} (acid compounds are not lacking) in rainwater observed here indicate a neutralization of acidity. The strong correlations of the acidic ions (SO_4^{2-} and NO_3^-) with cations further support neutralization (Table S2). Based on the VWM concentrations, the FA value of the HR and LR are calculated as 0.035 and 0.014, respectively, indicating that roughly 96.5% and 98.6% of rainwater acidity in the two sites is neutralized by alkaline matter. The calculated NF values for NH_4^+, Ca^{2+}, Mg^{2+}, and K^+ are 0.57, 0.49, 0.10, and 0.06, respectively, in HR rainwater samples, while the respective NF values are 0.73, 0.68, 0.09, and 0.06 in LR rainwater samples. These results indicate that NH_4^+ is the dominant cause of acid neutralization in the rainwater at both sites, and Ca^{2+} is the secondary cause, whereas the neutralization by Mg^{2+} and K^+ is insignificant. Compared with other areas, the NF values for NH_4^+ of HR and LR are higher than those of Chengdu (0.45) (Wang and Han, 2011) and Three Gorges Reservoir (0.39) (Wu and Han, 2015), revealing the important contribution of NH_3 emission driven by agriculture to acid neutralization of rainwater in this karst depression.

3.2. Sources of major ions in rainwater

The correlation coefficients among ions in rainwater of HR and LR are calculated and shown in Table S2. Positive correlations are observed between SO_4^{2-} 4and NO_3^- in both sites (R = 0.65 for HR and 0.73 for LR), as are expected because of the similarity of their atmospheric chemical behaviours and the co-emission sources for their precursors such as SO_2 and NO_x (Xiao, 2016). Strong correlations are also found between windblown dust species Ca^{2+} and Mg^{2+} (R = 0.76 for HR and 0.77 for LR), revealing the terrestrial source of these ions, which is consistent with the extensive development of carbonate rocks in the study area (Lü et al., 2017). Similarly, the sea-salt ions Na^+ and Cl^- also show significant correlations, reflecting a common marine source (Zhang et al., 2012; Rao et al., 2017). Positive correlations observed between other ions (e.g., SO_4^{2-} and Ca^{2+}, SO_4^{2-} and Mg^{2+}, NO_3^- and Ca^{2+}, NO_3^- and Mg^{2+}, SO_4^{2-} and NH_4^+) are considered to be the result of atmospheric neutralizing reactions of the acids (H_2SO_4 and HNO_3) with alkaline compounds (e.g., $CaCO_3$ and $MgCO_3$ exist in suspended fine particles). However, the correlations of NO_3^- and NH_4^+ are insignificant, indicating that the NH_3 reacts preferentially with H_2SO_4 in atmosphere (Wu et al., 2012).

Variations of the ionic compositions are also shown in the ternary diagrams (Fig. 3). Compared with the Cl^--enriched rainwater in marine areas (samples are plotted on the Cl^- end in the ternary diagrams) (Xiao et al., 2016), the anions of HR and LR rainwater samples are basically all scattered on the line between SO_4^{2-} and NO_3^- (Fig. 3a), indicating the controlling of anthropogenic emissions. Furthermore, the rainwater was seriously affected by mobile sources (e.g. vehicle exhaust), which has a low SO_4^{2-}/NO_3^- ratio (<1) (Arimoto et al., 1996). The rainwater samples in karst depression are inclined to the SO_4^{2-} end (Fig. 3a) and all the SO_4^{2-}/NO_3^- ratios are exceed 1 (except HR-10) with a mean value of 3.5 (Table S1), reflecting the fact that the rainwater is more influenced by the fixed emission sources than by mobile sources. Given the dilution of NO_x in the long-distance transport and the NO_x contributed by soil emission source (e.g., nitrification and denitrification), the mobile sources contribution to the rainwater NO_3^- is more muted. In cation ternary diagrams, the cations of HR and LR rainwater samples are scattered on the line between $Ca^{2+} + Mg^{2+}$ and NH_4^+ (Fig. 3b), showing that the rainwater cations are mainly controlled by the input of terrestrial sources and anthropogenic activities (Han and Liu, 2006; Han et al., 2010). In contrast, the input of marine sources has relatively little contribution to the total ionic composition of rainwater.

As shown in Fig. 4a, only a few rainwater samples of HR and LR have higher Cl^-/Na^+ ratios (except sample HR-17 with an extremely low Na^+ concentration), whereas other samples are lower than that of seawater (Berner and Berner, 1987). This suggests that the Cl^- contributed by anthropogenic sources is negligible, and the Na^+ from mineral weathering (e.g., silicate hydrolysis and mirabilite dissolution) may add to the atmosphere, resulting in a relative lower Cl^-/Na^+ ratio. Meanwhile, the low concentration and proportion of Cl^- and Na^+ (Table 2) caused by the dilution effect of marine-source input in the long-distance transport. SO_4^{2-} and NO_3^- are the sensitive indicators of anthropogenic pollution (Rao et al., 2017). The controlling of the two ions in rainwater by anthropogenic emissions has been mentioned above (Fig. 3a), which is further confirmed by the high SO_4^{2-}/Na^+ and NO_3^-/Na^+ ratios in Fig. 4a and b. The positive correlation of Cl^- with SO_4^{2-} and NO_3^- (Table S2) also indicates that these ions may have come from the same source.

There is a high NH_4^+/Na^+ ratio relative to the Cl^-/Na^+ ratio from

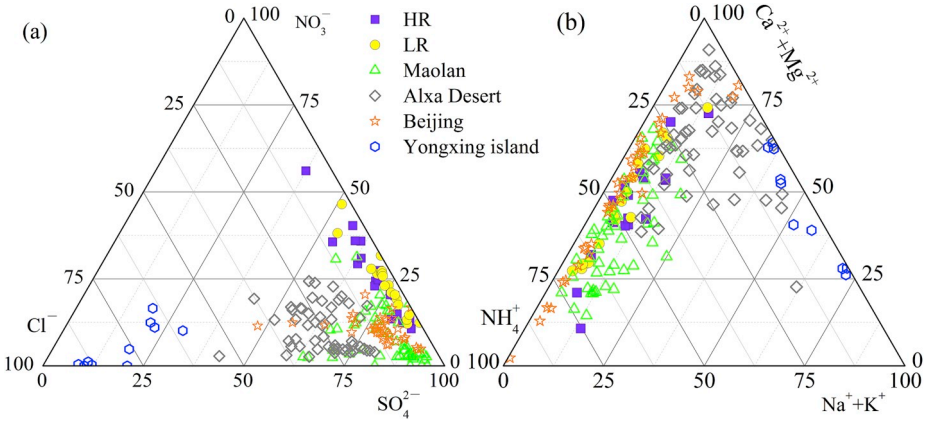

Fig. 3. Ternary diagrams showing ionic compositions, (a) anions, (b) cations. The data on rainwater observed in other areas in China are also shown. Data sources: Maolan (Han et al., 2010), Alxa Desert (Rao et al., 2017), Beijing (Xu et al., 2015), Yongxing Island (Xiao et al., 2016).

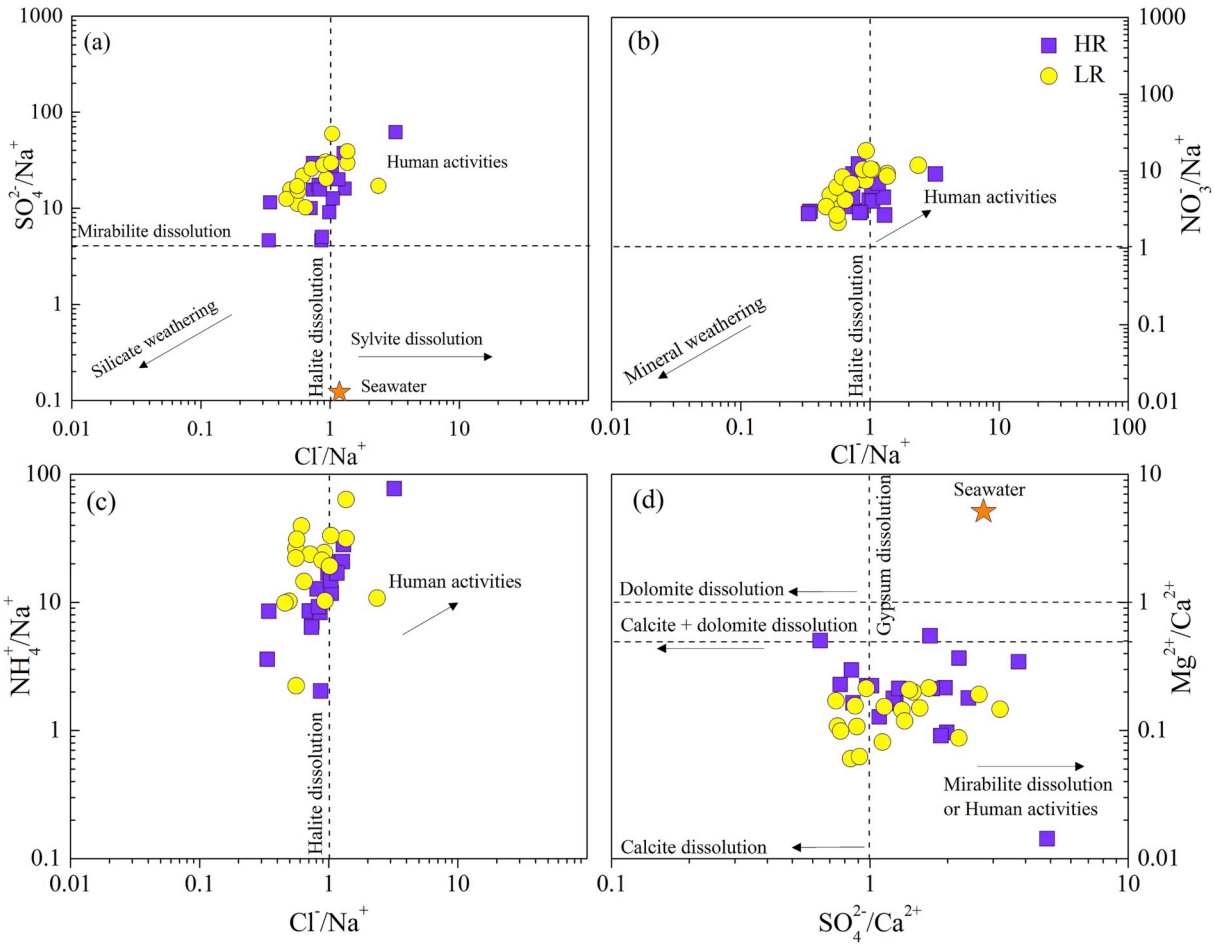

Fig. 4. The covariations of SO_4^{2-}/Na^+, NO_3^-/Na^+, NH_4^+/Na^+ with Cl^-/Na^+ and Mg^{2+}/Ca^{2+} with SO_4^{2-}/Ca^{2+} ratios (equivalent ratio) in rainwater at the HR and LR. The data on seawater is from Berner and Berner (1987), and the imaginary line (reference values) is from Rao et al. (2017).

Fig. 4c, but the strong correlation of NH_4^+ and Cl^- is only observed in HR ($R = 0.74$), while LR do not have a significant correlation (Table S2), suggesting NH_4^+ and Cl^- have different sources to some degree, at least in LR. Generally, the major source of rainwater NH_4^+ is derived from the dissolution of atmospheric NH_3 (g) emitted from fertilizer (urea, diammonium phosphate in this study area), livestock waste, and biomass burning (Jia and Chen, 2010; Liu et al., 2017), which are closely associated with agricultural activities (Russell et al., 1998; Zhao et al., 2009). This could be further confirmed by the effective indicator of NH_4^+/NO_3^- ratio (Xie et al., 2008; Lee et al., 2012). In this study, approximately 87% of the rainwater samples have a NH_4^+/NO_3^- ratio greater than 1 (ranging from 0.3 to 14.4 with a mean value of 3.5, Table S1), indicating that agriculture is the predominant source of rainwater NH_4^+ in the present study area. In addition, the relative high NH_4^+/NO_3^- ratio at LR indicated that more affected from agricultural activity than at HR. Furthermore, since there were few residents and the study period were undertaken during the rainy season, biomass is burned infrequently. NH_3 contribution from livestock waste and biomass can be ignored. Thus, the rainwater NH_4^+ mainly originated from the volatilization of fertilizer application during crop-growing. Thus, the NH_4^+ in rainwater originates mainly from the volatilization of fertilizer application in crop-growing seasons.

In Fig. 4d, the rainwater samples are scattered between two lines of calcite dissolution and [calcite + dolomite] dissolution with the Mg^{2+}/Ca^{2+} ratios are < 0.5, which implies that the Ca^{2+} and Mg^{2+} of rainwater are more affected by the calcite dissolution in atmospheric dust originating from the weathering and subsequent pedogenesis process (Lü et al., 2017).

The main sources of K^+ include sylvite (KCl, KNO_3, K_2SO_4), silicate weathering from local areas, and agricultural activities (biomass burning and fertilization) (Gaillardet et al., 1999; Rao et al., 2017). Sylvite was rarely observed in the study area and the distribution of silicates is also far less than that of carbonates. Thus, agricultural activities could be the main sources of rainwater K^+. Accordingly, for the farming activities, the sampling period (May to August) is not the period when biomass burning occurs, following the harvest, but the intensive fertilization period for crop-growing reveals the predominance of fertilization in rainwater K^+.

3.3. Controlling factors of ionic vertical distribution

Most ions (SO_4^{2-}, NH_4^+, Ca^{2+}, Mg^{2+}, K^+, and F^-) in LR present a higher VWM value than that in HR. Additionally, these ions found in LR rainwater had consistently higher concentrations in almost every rainfall event (Fig. 2). This type of ion concentration vertical variations in rainwater on a depression scale has not been reported in previous studies. Although the concentration of F^- usually reflect the influence of human activities (Zhang et al., 2019), most rainwater samples have low F^- concentrations (VWM values of 1.1 and 1.6 μeq/L in HR and XR, respectively) as well as the low K^+, Na^+, and Cl^- concentrations in the present study (Table 1). These ions account for 2.7% of the total ion concentrations. Considering the low concentrations found in this study, we did not discuss the vertical distribution of these ions (K^+, Na^+, F^-, and Cl^-).

As previously mentioned, NH_4^+ in rainwater primarily originates from the NH_3 volatilization of fertilizer during application. The NH_3(g)

has a relatively short diffusion distance in the atmosphere (Asman and van Jaarsveld, 1992), and could be washed out effectively by rainwater with a shorter atmospheric retention time (<2d) (Xiao and Liu, 2002). As the dominant cation of rainwater in this study (Table 1), the NH_4^+ concentration of rainwater shows an obvious vertical difference between the HR and LR (Fig. 2, $P < 0.01$). This may be caused by the relatively weak air convection movement within the depression, particularly the weak horizontal diffusion of air. Under such conditions, the NH_3(g) volatilized from agricultural activity, (nitrogen fertilization) tends to form a higher concentration area at the bottom of the depression, resulting in NH_3 (g) being captured by the frequent rainfall of the rainy season before it has fully diffused into the atmosphere (Fig. 5). Thus, the NH_4^+ concentration of rainwater was higher in LR. NH_4^+ is the primary N species in rainwater (Liu et al., 2017), the significant difference of NH_4^+ concentration of the rainwater between HR and LR is bound to cause the significant influence on the estimation of atmospheric N deposition, which would be discussed in section 3.4.

Ca^{2+} and Mg^{2+} are mainly of crust origin (Xiao et al., 2013; Rao et al., 2017), which are mainly from the carbonate weathering and subsequent pedogenesis process in the karst area. The HR site is located at the hilltop with less anthropogenic disturbance, where the vegetation is luxuriant (Liu et al., 2016; Hu et al., 2017). However, the LR site within the depression is cultivated land with intense agricultural activities (Zhao et al., 2018), and causes more Ca^{2+} and Mg^{2+} from surface soil to enter the atmosphere as suspended fine particles or atmospheric dust (Fig. 5), which could have been washed out by the rainfall and resulted in the higher Ca^{2+} and Mg^{2+} concentration of rainwater in LR than in HR (Table 1).

Although the VWM concentration of NO_3^- in LR was lower than that in HR (Table 1), the opposite trend (LR > HR) was observed in most rainfall events (Fig. 2). It is beyond the scope of this study to directly explain the difference of NO_3^- concentration in rainwater between the HR and LR collection sites.

To further understand the vertical variation in NO_3^- concentration, the nitrate isotopes ($\delta^{15}N$–NO_3^-) of rainwater were detected, which could be significantly affected by the source variations of NO_x (the precursor of NO_3^-) (Jia and Chen, 2010; Chen et al., 2019). Generally, the isotopic signature differences of several major NO_x (g) sources are significant, such as: coal combustion (+19.8 ± 5.2‰), vehicle exhaust (−2.5 ± 1.5‰), biomass burning (+12.5 ± 3.1‰), and, soil emission sources (−30.3 ± 9.4‰) (Li and Wang, 2008; Felix et al., 2012; Felix and Elliott, 2014; Walters et al., 2015; Fibiger and Hastings, 2016). In the present study, the NO_x source of biomass burning was lacking, and the NO_x sources of coal combustion or vehicle exhausts are unlikely to be of large variation after the long distance of diffusion.

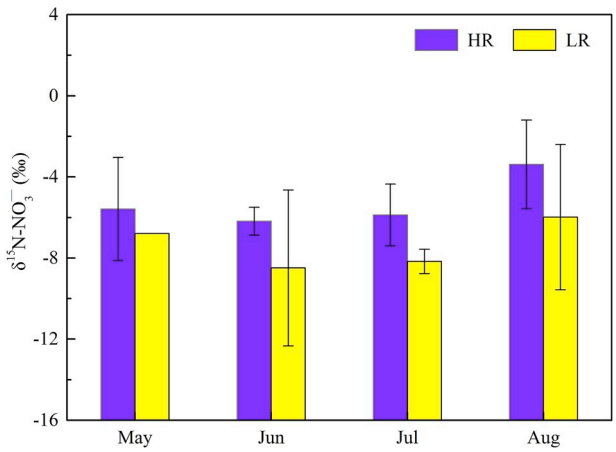

Fig. 6. The variation of $\delta^{15}N$–NO_3^- value in rainwater at the HR and LR.

As shown in Fig. 6, the mean $\delta^{15}N$–NO_3^- values of rainwater in LR were lower than that in HR, which indicated that the NO_x from soil emission sources (with the negative $\delta^{15}N$–NO_3^- value) are, most likely, captured by rainwater at LR. Thus, the vertical variations of $\delta^{15}N$–NO_3^- values between HR and LR might be controlled by soil emission NO_x (g) variations. In the rainy season, there are considerable amounts of NO_x introduced into the air via nitrification/denitrification in the alternately wet and dry soil, and these NO_x could accumulate in the depression due to the relatively weak air convection conditions (Fig. 5). Therefore, more ^{15}N-depleted NO_x from the soil emission are captured by rainfall in LR, and caused lower $\delta^{15}N$–NO_3^- values of rainwater in LR, which could partly explains that the vertical distribution of NO_3^- concentration is controlled by the soil emission NO_x.

There is obvious variation for SO_4^{2-} concentrations at two sites (Fig. 2). One possible cause is the differences in soil sulfur compounds emission at the two sites. Sulfur gas (e.g., hydrogen sulfide and carbonyl sulfide) released from surface soil can react with atmospheric oxygen to form SO_2 or SO_3 (Adams et al., 1981; Yang et al., 1998), which is then captured by rainwater and converted into SO_4^{2-}. These sulfur gases are preferentially released from the paddy soil with a low redox potential within the depression (LR) (Devai and DeLaune, 1995). This occurs particularly in the rainy season, which has the potential to promote

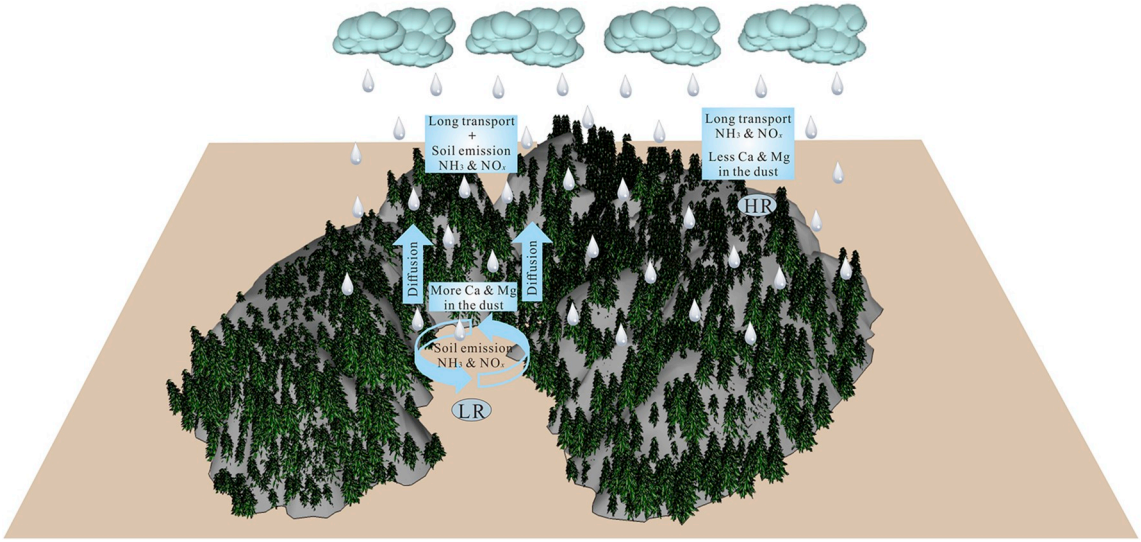

Fig. 5. The conceptual chart of materials cycle in karst depression.

microbial metabolism and increase the sulfur gas emission due to sticky weather (Goldan et al., 1987; Hirota et al., 2007). Furthermore, a previous study, on rice growth process monitoring showed that sulfur gas emission is mainly controlled by the application of fertilizer and in the growth of rice (Kanda et al., 1992).

Another potential factor was the direct absorption and assimilation of atmospheric SO_2 by plants. Compared with the paddy field, the luxuriant forest, consisting of secondary evergreen and deciduous broadleaved trees are developed on the hilltop area (HR), which has the capacity to absorb relatively more air SO_2 (Haneklaus et al., 2003). The two factors above could explain the vertical variation of rainwater SO_4^{2-} in the depression, to some extent.

3.4. Depression trapping effect on wet deposition flux

Generally, the wet deposition fluxes of ions are estimated by summing the product of monthly ion VWM concentration in rainwater and the monthly rainfall amount. In the plain area, NO_x, NH_3, and suspended fine particles could well diffuse between the underlying surface and the atmospheric boundary layer after these gases and particles are released into the atmosphere. Therefore, the wet deposition fluxes of the ions (NO_3^-, NH_4^+, Ca^{2+}, and Mg^{2+}) washed down by rainfall can be estimated more accurately by using the way mentioned above. Nevertheless, with the unique underlying surface (depression) and its local airflow movement, the ion concentrations of rainwater in the depression (LR) are different from that in the hilltops (HR), resulting in the inconsistent estimation of ion deposition fluxes (Fig. 7).

This result indicates that the influence of vertical variation of ion concentration in wet deposition on the estimation of wet deposition fluxes is significant (up to 80.6% for Ca^{2+}, 68.7% for NH_4^+, and 48.8% for SO_4^{2-}). Moreover, the wet deposition fluxes are positively correlated with rainfall amount, and most of the ions wet deposition fluxes are the highest in June, which reflects the importance of the rainy season (abundant rainfall) in annual wet deposition flux. Therefore, the depression trapping effect can affect the diffusion of gaseous materials (e.g., NO_x and NH_3) and suspended fine particles by local air flow movement on the atmospheric underlying surface. This accounts for the variations in ion concentration of rainwater between the LR and HR collection sites in this study, and affects the estimation of wet deposition fluxes.

The effect of the difference of wet deposition fluxes caused by the depression trapping effect mentioned above on material migration by runoff or cycle and associated environmental effect are vital important. Take nitrogen for example, aquatic ecosystems can receive N from direct atmospheric deposition on open water bodies or from N transported caused by N deposition on terrestrial ecosystem (Gao et al., 2019; Liu et al., 2019). If the N deposition flux from the top of Tianlong hill (HR) is applied to estimate the nitrogen cycle mass balance within the depression scale, then the N level of atmospheric input to the earth surface will be underestimated. On the contrary, if the N deposition flux of the LR is used to estimate, it will be overestimated. The recent study using online sensor technology has shown that N export from present studied area is 30.2 kg N/hm^2, of which 87.5% is from May to August (Yue et al., 2019). In the rainy season (May to August), the inorganic N ($NH_4^+ + NO_3^-$) input of rainwater to earth surface are 3.7 kg N/hm^2 at HR and 5.3 kg N/hm^2 (Fig. 7), which are 14.1% and 20.0% of the catchment area loading of inorganic N export in the rainy season, respectively. Thus, the contribution of wet deposition to the N export by stream within catchment cannot be ignored. Accurate precision this contribution is necessary for N cycle.

Previous studies have also concluded that the influence of different types of atmospheric underlying surface (orographic barriers) on pollutant diffusion is significantly different (Jazcilevich et al., 2002; He et al., 2017; Szép et al., 2019). Consequently, the depression trapping effect should be more considered in further research of atmospheric wet deposition, particularly in the karst areas with a diverse topography, such as depressions and peak clusters.

4. Conclusions

Rainwater samples in a karst agricultural depression were investigated systematically in order to explore the major ionic composition, sources, and ionic vertical distribution of rainwater during the rainy season. Subsequently, the effects of topography (depression in this study) on wet deposition fluxes were estimated. The main results are as follows:

The pH values of rainwater of the karst agricultural depression ranged from 4.8 to 6.9. Most samples were not identified as acid precipitation due to the result of neutralization caused by alkaline substances (NH_4^+ and Ca^{2+}). NH_4^+, Ca^{2+}, and NO_3^- dominated, accounting for

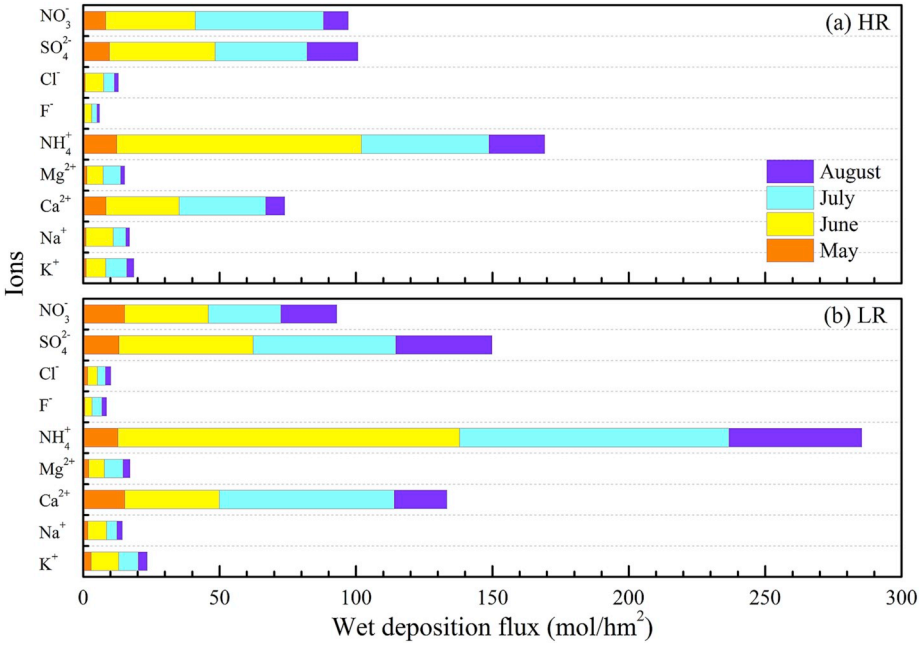

Fig. 7. Wet deposition fluxes of ions at the HR (a) and LR (b) in the karst agricultural depression.

>87% (average) of the total ions at the two sites. Major ion VWM concentrations decreased in the order of $SO_4^{2-} > NH_4^+ > Ca^{2+} > NO_3^- > Mg^{2+} > K^+ > Na^+ > Cl^- > F^-$ at both sites.

Anions were controlled predominantly by anthropogenic emission sources, while cations originated from both terrestrial sources and anthropogenic activity. The depression trapping effect of several ions (NH_4^+, NO_3^-, Ca^{2+}, Mg^{2+}, and SO_4^{2-}) was controlled by the relatively weak air convection movement within the depression and the differences in human interference at the two sites. This could have significantly affected the estimation of wet deposition fluxes, by up to 80.6% (Ca^{2+}) and 68.7% (NH_4^+). The higher frequency and long time scale sampling are required in the future studies to further explore the vertical distribution of rainwater chemistry and to better quantify the wet deposition flux.

Declaration of competing interest

The authors declare that they have no known competing financialinterestsor personal relationships that could have appeared to influence the work reported in this paper.

Acknowledgments

This work was supported by the National Natural Science Foundation of China, China [grant numbers 41571130072, 41861144026]; Natural Environment Research Council, United Kingdom [grant number NE/N007425/1]; the National Key R&D Program of China, China [grant number 2016YFA0601002]; and the Independent Innovative Foundation of Tianjin University, China [grant number 2019XZS-0016].

Appendix A. Supplementary data

Supplementary data to this article can be found online at https://doi.org/10.1016/j.atmosenv.2019.116998.

References

Adams, D.F., Farwell, S.O., Robinson, E., Pack, M.R., Bamesberger, W.L., 1981. Biogenic sulfur source strengths. Environ. Sci. Technol. 15, 1493–1498.
Arimoto, R., Duce, R.A., Savoie, D.L., Prospero, J.M., Talbot, R., Cullen, J.D., Tomza, U., Lewis, N.F., Ray, B.J., 1996. Relationships among aerosol constituents from Asia and the North Pacific during PEM-West A. J. Geophys. Res. Atmos. 101, 2011–2024.
Asman, W.A.H., van Jaarsveld, H.A., 1992. A variable-resolution transport model applied for NHχ in Europe. Atmos. Environ. Part A. General Topics 26, 445–464.
Balasubramanian, R., Victor, T., Chun, N., 2001. Chemical and statistical analysis of precipitation in Singapore. Water Air Soil Pollut. 130, 451–456.
Berner, E.K., Berner, R.A., 1987. Global Water Cycle: Geochemistry and Environment. Prentice-Hall, New York.
Chen, F., Lao, Q., Jia, G., Chen, C., Zhu, Q., Zhou, X., 2019. Seasonal variations of nitrate dual isotopes in wet deposition in a tropical city in China. Atmos. Environ. 196, 1–9.
Chen, X., Chen, C., Hao, Q., Zhang, Z., Shi, P., 2008. Simulation of rainfall-underground outflow responses of a karstic watershed in Southwest China with an artificial neural network. Water Sci.Eng. 1, 1–9.
Dai, Q.H., Peng, X.D., Wang, P.J., Li, C.L., Shao, H.B., 2018. Surface erosion and underground leakage of yellow soil on slopes in karst regions of southwest China. Land Degrad. Dev. 29, 2438–2448.
Devai, I., DeLaune, R.D., 1995. Formation of volatile sulfur compounds in salt marsh sediment as influenced by soil redox condition. Org. Geochem. 23, 283–287.
Felix, J.D., Elliott, E.M., 2014. Isotopic composition of passively collected nitrogen dioxide emissions: vehicle, soil and livestock source signatures. Atmos. Environ. 92, 359–366.
Felix, J.D., Elliott, E.M., Shaw, S.L., 2012. Nitrogen isotopic composition of coal-fired power plant NOx: influence of emission controls and implications for global emission inventories. Environ. Sci. Technol. 46, 3528–3535.
Fibiger, D.L., Hastings, M.G., 2016. First measurements of the nitrogen isotopic composition of NOx from biomass burning. Environ. Sci. Technol. 50, 11569–11574.
Gaillardet, J., Dupré, B., Louvat, P., Allègre, C.J., 1999. Global silicate weathering and CO_2 consumption rates deduced from the chemistry of large rivers. Chem. Geol. 159, 3–30.
Galloway, J.N., Savoie, D.L., Keene, W.C., Prospero, J.M., 1993. The temporal and spatial variability of scavenging ratios for NSS sulfate, nitrate, methanesulfonate and sodium in the Atmosphere over the North Atlantic Ocean. Atmos. Environ. Part A. General Topics 27, 235–250.
Galloway, J.N., Townsend, A.R., Erisman, J.W., Bekunda, M., Cai, Z., Freney, J.R., Martinelli, L.A., Seitzinger, S.P., Sutton, M.A., 2008. Transformation of the nitrogen cycle: recent trends, questions, and potential solutions. Science 320, 889.
Gao, Y., Hao, Z., Yang, T., He, N., Wen, X., Yu, G., 2017. Effects of atmospheric reactive phosphorus deposition on phosphorus transport in a subtropical watershed: a Chinese case study. Environ. Pollut. 226, 69–78.
Gao, Y., Zhou, F., Ciais, P., Miao, C., Yang, T., Jia, Y., Zhou, X., Klaus, B.-B., Yu, G., Yang, T., 2019. Human activities aggravate nitrogen deposition pollution to inland water over China. Natl. Sci. Rev. https://doi.org/10.1093/nsr/nwz073.
Goldan, P.D., Kuster, W.C., Albritton, D.L., Fehsenfeld, F.C., 1987. The measurement of natural sulfur emissions from soils and vegetation: three sites in the Eastern United States revisited. J. Atmos. Chem. 5, 439–467.
Han, G., Liu, C.-Q., 2006. Strontium isotope and major ion chemistry of the rainwaters from Guiyang, Guizhou Province, China. Sci. Total Environ. 364, 165–174.
Han, G., Tang, Y., Wu, Q., Tan, Q., 2010. Chemical and strontium isotope characterization of rainwater in karst virgin forest, Southwest China. Atmos. Environ. 44, 174–181.
Han, G., Song, Z., Tang, Y., Wu, Q., Wang, Z., 2019. Ca and Sr isotope compositions of rainwater from Guiyang city, Southwest China: implication for the sources of atmospheric aerosols and their seasonal variations. Atmos. Environ. 214, 116854.
Hao, Z., Gao, Y., Yang, T., Tian, J., 2017. Atmospheric wet deposition of nitrogen in a subtropical watershed in China: characteristics of and impacts on surface water quality. Environ. Sci. Pollut. Control Ser. 24, 8489–8503.
Haneklaus, S., Bloem, E., Schnug, E., 2003. The global sulphur cycle and its links to plant environment. In: Abrol, Y.P., Ahmad, A. (Eds.), Sulphur in Plants. Springer Netherlands, Dordrecht, pp. 1–28.
Hao, J., Duan, L., Zhou, X., Fu, L., 2001. Application of a LRT model to acid rain control in China. Environ. Sci. Technol. 35, 3407.
He, X., Ye, X.-m., Ma, W.-l., Wang, C.-g., 2017. Study of the effects of urban underlying surface changing on the air pollution diffusion in Hangzhou. Sci. Technol. Eng. 17, 122–130 (in Chinese).
Hirota, M., Senga, Y., Seike, Y., Nohara, S., Kunii, H., 2007. Fluxes of carbon dioxide, methane and nitrous oxide in two contrastive fringing zones of coastal lagoon, Lake Nakaumi, Japan. Chemosphere 68, 597–603.
Hu, G., Zhang, Z., Cheng, A., Liu, L., Wu, Y., Ni, J., 2017. Characterizing and analyzing stand spatial structure of a northern subtropical karst secondary forest in Tianlong Mountain of central Guizhou province, China. Earth Environ. 45, 25–31 (in Chinese).
Jazcilevich, A.D., García, A.n.R., Ruíz-Suárez, L.G., 2002. A modeling study of air pollution modulation through land-use change in the Valley of Mexico. Atmos. Environ. 36, 2297–2307.
Jia, G., Chen, F., 2010. Monthly variations in nitrogen isotopes of ammonium and nitrate in wet deposition at Guangzhou, south China. Atmos. Environ. 44, 2309–2315.
Kanda, K.-i., Tsuruta, H., Minami, K., 1992. Emission of dimethyl sulfide, carbonyl sulfide, and carbon bisulfide from paddy fields. Soil Sci. Plant Nutr. 38, 709–716.
Lü, P., Han, G., Wu, Q., 2017. Chemical characteristics of rainwater in karst rural areas, Guizhou Province, Southwest China. Acta Geochimica 36, 572–576.
Larssen, T., Lydersen, E., Tang, D., He, Y., Gao, J., Liu, H., Duan, L., Seip, H.M., Vogt, R. D., Mulder, J., Shao, M., Wang, Y., Shang, H., Zhang, X., Solberg, S., Aas, W., Okland, T., Eilertsen, O., Angell, V., Li, Q., Zhao, D., Xiang, R., Xiao, J., Luo, J., 2006. Acid rain in China. Environ. Sci. Technol. 40, 418–425.
Lee, K.-S., Lee, D.-S., Lim, S.-S., Kwak, J.-H., Jeon, B.-J., Lee, S.-I., Lee, S.-M., Choi, W.-J., 2012. Nitrogen isotope ratios of dissolved organic nitrogen in wet precipitation in a metropolis surrounded by agricultural areas in southern Korea. Agric. Ecosyst. Environ. 159, 161–169.
Li, C., Kang, S., Zhang, Q., Kaspari, S., 2007. Major ionic composition of precipitation in the Nam Co region, Central Tibetan Plateau. Atmos. Res. 85, 351–360.
Li, D., Wang, X., 2008. Nitrogen isotopic signature of soil-released nitric oxide (NO) after fertilizer application. Atmos. Environ. 42, 4747–4754.
Liu, C., Liu, Y., Guo, K., Wang, S., Liu, H., Zhao, H., Qiao, X., Hou, D., Li, S., 2016. Aboveground carbon stock, allocation and sequestration potential during vegetation recovery in the karst region of southwestern China: a case study at a watershed scale. Agric. Ecosyst. Environ. 235, 91–100.
Liu, M., Han, G., Zhang, Q., Song, Z., 2019. Variations and indications of $\delta^{13}C_{SOC}$ and $\delta^{15}N_{SON}$ in soil profiles in karst critical zone observatory (CZO), southwest China. Sustainability 11, 2144.
Liu, X.Y., Xiao, H.W., Xiao, H.Y., Song, W., Sun, X.C., Zheng, X.D., Liu, C.Q., Koba, K., 2017. Stable isotope analyses of precipitation nitrogen sources in Guiyang, southwestern China. Environ. Pollut. 230, 486.
Lu, X., Li, L.Y., Li, N., Yang, G., Luo, D., Chen, J., 2011. Chemical characteristics of spring rainwater of Xi'an city, NW China. Atmos. Environ. 45, 5058–5063.
Ma, M., Gao, Y., Song, X., Green, S.M., Xiong, B., Dungait, J.A.J., Peng, T., Quine, T.A., Wen, X., He, N., 2018. Migration and leaching characteristics of base cation: indicating environmental effects on soil alkalinity in a karst area. Environ. Sci. Pollut. Control Ser. 25, 20899–20910.
McIlvin, M.R., Casciotti, K.L., 2011. Technical updates to the bacterial method for nitrate isotopic analyses. Anal. Chem. 83, 1850–1856.
Mouli, P.C., Mohan, S.V., JayaramaReddya, S., 2005. Rainwater chemistry at a regional representative urban site: influence of terrestrial sources on ionic composition. Atmos. Environ. 39, 999–1008.
Possanzini, M., Buttini, P., Di, P.V., 1988. Characterization of a rural area in terms of dry and wet deposition. Sci. Total Environ. 74, 111–120.
Rao, W., Han, G., Tan, H., Jiang, S., 2015. Chemical and Sr isotopic compositions of rainwater on the ordos desert plateau, northwest China. Environ. Earth Sci. 74, 5759–5771.

Rao, W., Han, G., Tan, H., Jin, K., Wang, S., Chen, T., 2017. Chemical and Sr isotopic characteristics of rainwater on the Alxa Desert Plateau, North China: implication for air quality and ion sources. Atmos. Res. 193, 163–172.
Russell, K.M., Galloway, J.N., Macko, S.A., Moody, J.L., Scudlark, J.R., 1998. Sources of nitrogen in wet deposition to the Chesapeake Bay region. Atmos. Environ. 32, 3923–3927.
Song, X., Gao, Y., Green, S.M., Dungait, J.A.J., Peng, T., Quine, T.A., Xiong, B., Wen, X., He, N., 2017. Nitrogen loss from karst area in China in recent 50 years: an in-situ simulated rainfall experiment's assessment. Ecol. Evol. 7, 10131–10142.
Špičková, J., Dobešová, I., Vach, M., Skřivan, P., Mihaljevič, M., Burian, M., 2008. The influence of the limestone-quarry Čertovy schody (Czech Republic) on the precipitation chemistry and atmospheric deposition. Chemie der Erde - Geochemistry 68, 105–115.
Szép, R., Mateescu, E., Niță, I.-A., Birsan, M.-V., Bodor, Z., Keresztesi, Á., 2018. Effects of the Eastern Carpathians on atmospheric circulations and precipitation chemistry from 2006 to 2016 at four monitoring stations (Eastern Carpathians, Romania). Atmos. Res. 214, 311–328.
Szép, R., Bodor, Z., Miklóssy, I., Niță, I.A., Oprea, O.A., Keresztesi, Á., 2019. Influence of peat fires on the rainwater chemistry in intra-mountain basins with specific atmospheric circulations (Eastern Carpathians, Romania). Sci. Total Environ. 647, 275–289.
Tang, Y., Han, G., 2019. Seasonal variation and quality assessment of the major and trace elements of atmospheric dust in a typical karst city, southwest China. Int. J. Environ. Res. Public Health 16.
Tao, Y., Mi, S., Zhou, S., Wang, S., Xie, X., 2014. Air pollution and hospital admissions for respiratory diseases in Lanzhou, China. Environ. Pollut. 185, 196–201.
Walters, W.W., Goodwin, S.R., Michalski, G., 2015. Nitrogen stable isotope composition ($\delta^{15}N$) of vehicle-emitted NOx. Environ. Sci. Technol. 49, 2278–2285.
Wang, H., Han, G., 2011. Chemical composition of rainwater and anthropogenic influences in Chengdu, Southwest China. Atmos. Res. 99, 190–196.
Wei, J., Li, Z., Peng, Y., Sun, L., 2019. MODIS Collection 6.1 aerosol optical depth products over land and ocean: validation and comparison. Atmos. Environ. 201, 428–440.
Wu, Q., Han, G., 2015. Sulfur isotope and chemical composition of the rainwater at the Three Gorges Reservoir. Atmos. Res. 155, 130–140.
Wu, Q., Han, G., Tao, F., Tang, Y., 2012. Chemical composition of rainwater in a karstic agricultural area, Southwest China: the impact of urbanization. Atmos. Res. 111, 71–78.
Xiao, H.-W., Long, A.-m., Xie, L.-h., Xiao, H.-Y., Liu, C.-q., 2014. Chemical characteristics of precipitation in south China sea. Environ. Sci. 35, 475–480 (in Chinese).
Xiao, H.-W., Xiao, H.-Y., Zhang, Z.-y., Wang, Y.-L., Long, A.-m., Liu, C.Q., 2016. Chemical characteristics and source apportionment of atmospheric precipitation in Yongxing Island. China Environ. Sci. 36, 3237–3244 (in Chinese).
Xiao, H.W., Xiao, H.Y., Long, A.M., Wang, Y.L., Liu, C.Q., 2013. Chemical composition and source apportionment of rainwater at Guiyang, SW China. J. Atmos. Chem. 70, 269–281.
Xiao, H.Y., Liu, C.Q., 2002. Sources of nitrogen and sulfur in wet deposition at Guiyang, southwest China. Atmos. Environ. 36, 5121–5130.
Xiao, J., 2016. Chemical composition and source identification of rainwater constituents at an urban site in Xi'an. Environ. Earth Sci. 75, 209.
Xiao, J., Jin, Z.D., Wang, J., Zhang, F., 2015. Hydrochemical characteristics, controlling factors and solute sources of groundwater within the Tarim River Basin in the extreme arid region, NW Tibetan Plateau. Quat. Int. 380–381, 237–246.
Xie, Y., Xiong, Z., Xing, G., Yan, X., Shi, S., Sun, G., Zhu, Z., 2008. Source of nitrogen in wet deposition to a rice agroecosystem at Tai lake region. Atmos. Environ. 42, 5182–5192.
Xu, Z., Wu, Y., Liu, W.-J., Liang, C.-S., Ji, J., Zhao, T., Zhang, X., 2015. Chemical composition of rainwater and the acid neutralizing effect at Beijing and Chizhou city, China. Atmos. Res. 164–165, 278–285.
Yan, Y., Dai, Q., Yuan, Y., Peng, X., Zhao, L., Yang, J., 2018. Effects of rainfall intensity on runoff and sediment yields on bare slopes in a karst area, SW China. Geoderma 330, 30–40.
Yang, Z., Kong, L., Zhang, J., Wang, L., Xi, S., 1998. Emission of biogenic sulfur gases from Chinese rice paddies. Sci. Total Environ. 224, 1–8.
Yu, S., Kuo, Y.-M., Du, W., He, S., Sun, P.-A., Yuan, Y., Li, R., Li, Y., 2015. The hydrochemistry properties of precipitation in karst tourism city (Guilin), Southwest China. Environ. Earth Sci. 74, 1061–1069.
Yue, F.J., Li, S.L., Liu, C.Q., Lang, Y.C., Ding, H., 2015. Sources and transport of nitrate constrained by the isotopic technique in a karst catchment: an example from Southwest China. Hydrol. Process. 29, 1883–1893.
Yue, F.J., Li, S.L., Zhong, J., Liu, J., 2018. Evaluation of factors driving seasonal nitrate variations in surface and underground systems of a karst catchment. Vadose Zone J. 17 https://doi.org/10.2136/vzj2017.04.0071, 170071.
Yue, F.J., Waldron, S., Li, S.L., Wang, Z.J., Zeng, J., Xu, S., Zhang, Z.C., Oliver, D.M., 2019. Land use interacts with changes in catchment hydrology to generate chronic nitrate pollution in karst waters and strong seasonality in excess nitrate export. Sci. Total Environ. https://doi.org/10.1016/j.scitotenv.2019.134062.
Zeng, J., Han, G., Zhu, J.M., 2019. Seasonal and spatial variation of Mo isotope compositions in headwater stream of Xijiang river draining the carbonate Terrain, southwest China. Water 11, 1076.
Zhang, X., Jiang, H., Zhang, Q., Zhang, X., 2012. Chemical characteristics of rainwater in northeast China, a case study of Dalian. Atmos. Res. 116, 151–160.
Zhang, X., Xu, Z., Liu, W., Moon, S., Zhao, T., Zhou, X., Zhang, J., Wu, Y., Jiang, H., Zhou, L., 2019. Hydro-geochemical and Sr isotope characteristics of the Yalong river basin, eastern Tibetan plateau: implications for chemical weathering and controlling factors. Geochem. Geophys. Geosyst. https://doi.org/10.1029/2018GC007769.
Zhang, Y., LEE, X., Cao, F., Huang, D., 2011. Seasonal variation and sources of low molecular weight organic acids in precipitation in the rural area of Anshun. Chin. Sci. Bull. 56, 1005–1010.
Zhang, Z., Chen, X., Soulsby, C., 2017. Catchment-scale conceptual modelling of water and solute transport in the dual flow system of the karst critical zone. Hydrol. Process. 31, 3421–3436.
Zhao, M., Hu, Y., Zeng, C., Liu, Z., Yang, R., Chen, B., 2018. Effects of land cover on variations in stable hydrogen and oxygen isotopes in karst groundwater: a comparative study of three karst catchments in Guizhou Province, Southwest China. J. Hydrol. 565, 374–385.
Zhao, X., Yan, X., Xiong, Z., Xie, Y., Xing, G., Shi, S., Zhu, Z., 2009. Spatial and temporal variation of inorganic nitrogen wet deposition to the Yangtze River delta region, China. Water Air Soil Pollut. 203, 277–289.
Zhao, Z., Tian, L., Fischer, E., Li, Z., Jiao, K., 2008. Study of chemical composition of precipitation at an alpine site and a rural site in the Urumqi River Valley, Eastern Tien Shan, China. Atmos. Environ. 42, 8934–8942.
Zhou, X., Xu, Z., Liu, W., Wu, Y., Zhao, T., Jiang, H., Zhang, X., Zhang, J., Zhou, L., Wang, Y., 2019. Chemical composition of precipitation in Shenzhen, a coastal mega-city in South China: influence of urbanization and anthropogenic activities on acidity and ionic composition. Sci. Total Environ. 662, 218–226.